Differential uplift and tilt of Pleistocene reef platforms and Quaternary slip rate on the Morne-Piton normal fault (Guadeloupe, French West Indies)

N. Feuillet, P. Tapponnier, I. Manighetti, B. Villemant, G. C. P. King

Differential uplift and tilt of Pleistocene reef platforms and Quaternary slip rate on the Morne-Piton normal fault (Guadeloupe, French West Indies)

N. Feuillet,[1] P. Tapponnier, and I. Manighetti[2]

Institut De Physique du Globe de Paris, Laboratoire de Tectonique et Mécanique de la Lithosphère, Paris, France

B. Villemant

Université Pierre et Marie Curie and Institut De Physique du Globe de Paris, Laboratoire de Géochimie des Systèmes Volcaniques, CNRS UMR 7040, Paris, France

G. C. P. King

Institut De Physique du Globe de Paris, Laboratoire de Tectonique et Mécanique de la Lithosphère, Paris, France

Received 14 March 2003; revised 24 October 2003; accepted 31 October 2003; published 14 February 2004.

[1] The Guadeloupe islands are cut by normal faults that accommodate oblique convergence between the North American and Caribbean plates. Such faults are responsible for part of the shallow seismicity and have produced $M \geq 5$ damaging earthquakes. To better assess the seismic hazard in Guadeloupe, we quantify the slip rate on one of the largest fault (Morne-Piton). This roughly E-W fault crosses the island of Marie-Galante and uplifts a flight of reef terraces. From geomorphic analysis, we mapped three main terraces. New U/Th datings show that they formed during the latest interglacials, ~120 and ~240 kyr ago. Correlation with SPECMAP isotopic records implies that the Marie-Galante plateau emerged during the ~330 ka highstand. Topographic profiles show that the terraces and the plateau are deformed by faulting. Elastic modeling of their shape constrains the geometry of the fault (70–80° dip, 5 km depth) and its slip rate (0.5 ± 0.2 mm/yr). Given its length (50 km), depth, and slip rate, this fault might produce maximum $M \sim 6.5$ earthquakes with a recurrence time of 1400 to 3300 years, or more likely smaller events such as the $M \sim 5.5$ 16 May 1851 and 3 August 1992 shocks that might recur every 400 to 1000 years. We also show that all the islands and terraces are tilted westward perpendicularly to the trench. La Désirade closest to the trench is uplifted by 276 m, whereas subsidence (−70 m) is observed 10 km east of the volcanic arc. This tilt probably resulted from a transient deformation episode at the subduction interface that predated the late Pleistocene. *INDEX TERMS:* 3210 Mathematical Geophysics: Modeling; 7230 Seismology: Seismicity and seismotectonics; 8010 Structural Geology: Fractures and faults; 8110 Tectonophysics: Continental tectonics—general (0905); *KEYWORDS:* active normal faulting, reef terraces, elastic modeling

Citation: Feuillet, N., P. Tapponnier, I. Manighetti, B. Villemant, and G. C. P. King (2004), Differential uplift and tilt of Pleistocene reef platforms and Quaternary slip rate on the Morne-Piton normal fault (Guadeloupe, French West Indies), *J. Geophys. Res.*, *109*, B02404, doi:10.1029/2003JB002496.

1. Introduction

[2] The northern part of the Lesser Antilles arc is the site of trench parallel extension, accommodating the oblique convergence between the North American and Caribbean plates [*Feuillet et al.*, 2001, 2002] (Figure 1 inset). Such extension gives rise to active, oblique, normal faults that cut the northeastern edge of the Caribbean plate. Between Dominica and Antigua, they form two distinct sets (Figure 1). Faults belonging to the first set bound arc-perpendicular grabens or half grabens that offset the outer arc reef platforms of Grande-Terre, Marie-Galante, and La Désirade. Faults of the other set are roughly N140°E striking, en échelon, oblique normal faults that accommodate left-lateral slip along the inner, volcanic islands between Les Saintes and Nevis. The overall arrangement of faulting, at the scale of the arc, is a sinistral horsetail. Such active faults are responsible for several historical earthquakes as

[1]Now at Istituto Nazionale di Geofisica e Vulcanologia, Rome, Italy.
[2]Now at Department of Earth Sciences, University of Southern California, Los Angeles, California, USA.

0148-0227/04/2003JB002496$09.00

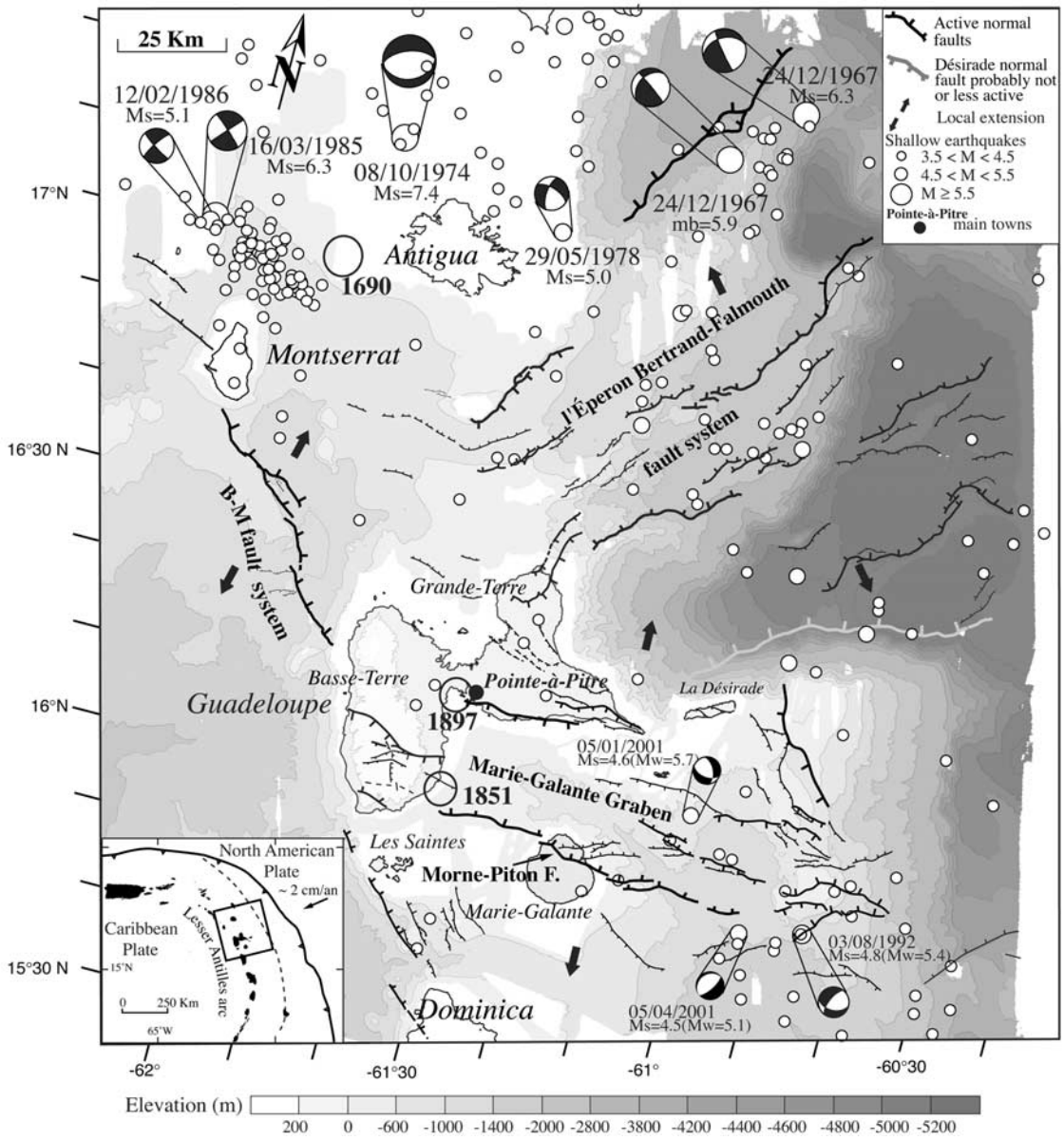

Figure 1. Seismotectonic map of the northern Lesser Antilles arc between Dominica and Antigua. Topography from French Institut Géographique National DEM. High-resolution multibeam bathymetry redrawn from AGUADOMAR cruise DEM (N/O l'Atalante, December 1998 to January 1999) [see *Feuillet*, 2000; *Deplus et al.*, 2001]. Active faults (black lines with ticks, with thicker lines for higher scarps) from *Feuillet* [2000] and *Feuillet et al.* [2001, 2002]. Double black arrows, local direction of extension deduced from fault geometry. White dots, 1981–1998 shallow (<30 km) seismicity from bulletins of volcanologic observatories of Guadeloupe and Martinique (Institut de Physique du Globe de Paris). Focal mechanisms of main intraplate earthquakes with dates from *Dziewonski et al.* [2000] (see also the Harvard University online catalog available at http://www.seismology.harvard.edu/CMTsearch.html), *Stein et al.* [1982], and *McCann et al.* [1982]. Open circles, location of I $\geq$ VII earthquakes with dates from *Robson* [1964], *Feuillard* [1985], and *Bernard and Lambert* [1988]. Inset, geodynamic setting of the Lesser Antilles arc; black line with triangles, accretionary prism front thrust; dashed black line, main negative gravity anomaly corresponding to the lesser Antilles trench from *Bowin* [1976] as cited by *Bouysse and Westercamp* [1990]; black arrow, North American/Caribbean plates subduction vector with rate indicated in centimeters from *DeMets et al.* [2000]; Islands in black; box, location of Figure 1.

well as for part of the shallow instrumental seismicity. In the last 150 years, two events with intensity VII–VIII occurred near the Marie-Galante graben, on 29 April 1897 and 16 May 1851 [e.g., *Bernard and Lambert*, 1988]. The 10–15 km deep, M_s = 5.6, 3 August 1992 and M_s = 4.6, 5 January 2001 shocks have oblique focal mechanisms compatible with roughly N-S extension, and probably ruptured the graben faults. Farther north, the 16 march 1985, M_s = 6.3 Nevis earthquake [*Girardin et al.*, 1990] ruptured a left-lateral plane that probably marks the northwestward continuation

of the fault system identified between Basse-Terre and Montserrat. The biggest known event (M_s = 7.4), recorded on 8 October 1974, north of Antigua, occurred along a roughly E-NE striking, southeast dipping normal fault [*McCann et al.*, 1982] similar to those of the Eperon Bertrand-Falmouth system, northeast of Guadeloupe. Since some of these faults come close to a densely populated area (Pointe-à-Pitre), their existence implies additional seismic hazard besides that induced by earthquakes on the NAM/CAR subduction interface (e.g., 8 February 1843 [*Sainte-Claire Deville*, 1843; *Bernard and Lambert*, 1988]).

[3] In this paper, we seek to constrain better the mechanisms and rates of Quaternary deformation in the Guadeloupe archipelago. The study combines geomorphic analysis with mechanical modeling. We focused on the island of Marie-Galante, which is cut by the largest fault of the archipelago (Morne-Piton) [*Feuillet et al.*, 2002]. The fault uplifts a flight of marine reef terraces, and the fringing reefs along the southeastern shore of Marie-Galante. Such marine terraces approximate paleoshorelines and result from the interplay between global sea level changes and tectonic uplift [e.g., *Chappell*, 1974; *Lajoie*, 1986]. They can be used to improve quantitative understanding of throw rate, crustal rheology and earthquake mechanics [e.g., *Valensise and Ward*, 1991; *Armijo et al.*, 1996].

[4] Using 1/20,000 stereophotographs combined with 1/25,000 topographic maps, we accurately mapped the terrace's edges in the field. Topographic profiles of the elevations of their inner edges, which correspond to sea level highstands, were determined, showing the deformation of the terrace surfaces by tectonic processes. On the basis of new U/Th ages and stratigraphy, we correlate each level with the worldwide chronology of Pleistocene sea level changes. We model the shape of the Marie-Galante upper plateau and terraces as a result of response of an elastic half-space to slip along a dislocation. In doing so, we determine the cumulative slip responsible for the vertical surface displacements recorded by the terraces and the slip rate of the Morne-Piton fault. We also correct the Marie-Galante topography from the modeled topography, and deduce regional residual tilts perpendicular to the trench, that are likely related to subduction. Finally, we discuss the implications of our results in terms of seismic hazard.

2. Normal Faulting of Uplifted Coral Terraces in Marie-Galante

[5] The Morne-Piton fault, which is ~50 km long, limits the Marie-Galante graben to the south (Figure 1). It is composed of five 10 to 20 km long, N90 ± 30°E striking, north dipping segments arranged in a left-lateral échelon oriented approximately N100°E (Figure 2b). The onland segment, described in detail by *Feuillet et al.* [2002], separates the island of Marie-Galante in two parts (Figure 3). It exhibits a steep cumulative scarp, up to 130 m high, with a kink-shaped trace. The N140°E trending part of the kink is associated with smaller faults trending E-W to N60°E and probably accommodates a left-lateral component of slip. West of the island, the submarine segment of the fault cuts and offsets the Colombie bank by 10–90 m. East of the island, new bathymetric maps [*Feuillet*, 2000] show that the fault scarp reaches a height of 120 m and crosscuts the Marie-Galante canyon. The overall geometry of the Morne-Piton fault is compatible with a roughly N-S extension.

[6] The Plio-Pleistocene coral platform cut by the Morne-Piton fault is up to 200 m thick [*Andreieff et al.*, 1989; *Bouysse et al.*, 1993]. It is composed of two main units. The most important lower unit, more than 100 m thick, is made of the Plio-Pleistocene rhodolyth limestones that cap the entire island. The thinner (15–25 m) upper unit consists of Pleistocene polyps. It has been mapped only along the eastern border of the southern plateau of the island and at the base of the fault scarp, where only one small outcrop remains [*Bouysse et al.*, 1993]. The nature of the latter unit attests to a decrease of water depth. The surface of the southern plateau reaches a maximum elevation of 204 m near Ravine Carambole, close to the Morne-Piton fault (Figure 4). In addition to the plateau, the fault offsets a flight of marine terraces that hug the southeastern coast of Marie-Galante (Figure 5) and disappear, as does the fringing reef, north of the fault (Figure 3). Previous studies by *Lasserre* [1961], *De Reynal de Saint Michel* [1966], *Grellet and Sauret* [1988], and *Bouysse et al.* [1993] identified three main terraces, and *Battistini et al.* [1986] determined an Eemian U/Th age (~120 ka) for the lowest one, just north of Capesterre (Figure 3).

[7] It is now accepted that the uplifted marine terraces that form along a tectonically rising coast record the Pleistocene sequence of sea level highstands [e.g., *Mesollela et al.*, 1969; *Lajoie*, 1986]. They are erosional or depositional platforms that slope seaward by at most 10° and are backed by relict sea cliffs. Their ''inner edge,'' which is the intersection between the platform and the sea cliff, marks the shoreline angle that approximates the location of the paleo-sea level highstand (Figure 6). Such flights of terraces thus resemble flights of stairs, with the lowest terrace being the youngest [e.g., *Lajoie*, 1986; *Armijo et al.*, 1996].

[8] By combining the analysis of 1/20,000 scale, stereo pairs of aerial photographs and 1/25000 scale topographic maps of the French Institut Géographique National (IGN), we mapped the contours of both the inner and seaward edges (i.e., the top of the next, youngest sea cliff) for each terrace (Figures 3 and 4). The highest terrace T1 stands 120 m above sea level, on average. It is ~5 km long and up to ~100 m wide and extends between Morne Bel-air and Gros-Morne (Figure 4). It is interrupted by stream incisions in many places. The T2 terrace (Des Galets terrace), ~700 m wide, is less eroded and much broader than T1. It stands 50–70 m on average above sea level and is backed by a relict sea cliff 100 m high on average. It stretches from La Pointe Des Basses, southernmost tip of the island, to Anse-Piton and is ~15 km long. Its seaward edge is irregular, and does not follow the present-day shoreline. Between Pointe Des Basses and Ravine Carambole, it is divided into 10 main patches by small streams.

[9] The lowest terrace T4 (Capesterre terrace) is not incised by seaward flowing streams. It stands only 5 m above sea level on average, and extends all the way between Pointe Des Basses and Anse Piton. It is backed by the ~50 m high relict cliff that postdates the abandonment of T2. Its width ranges between 20 and 500 m. North of Morne à Boeuf, T4 shrinks to a narrow ledge, limited by a higher, steeper sea cliff with several notches visible in the field (Figure 4). This suggests locally faster uplift rates.

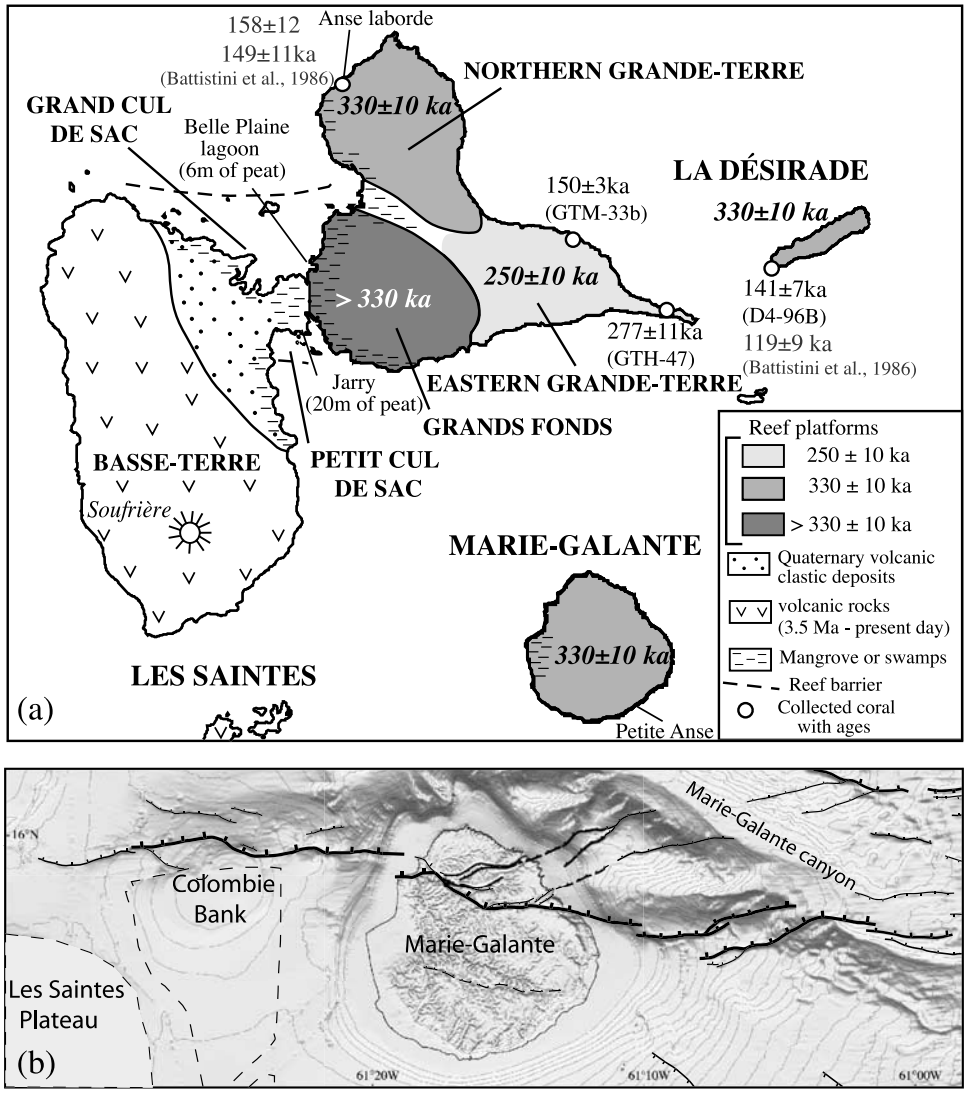

Figure 2. (a) Islands of Guadeloupe archipelago. Simplified geology on Basse-Terre from *Westercamp* [1980]. Ages (in bold italic) of Grande-Terre, Marie-Galante, and La Désirade reef platforms from this study, with older platforms in darker gray (see text). White dots, position, names, and U/Th ages of corals collected on the three reef islands for this study (ages in black, see Table 2a) and by *Battistini et al.* [1986] (ages in gray, see Table 2c). Mangrove repartition at Grande-Terre, swamps location at Marie-Galante and "Grand Cul de Sac" and "Petit Cul de Sac" reef barriers (indicated in dashed line) from French Institut Géographique National tourist map of Guadeloupe (scale 1:100,000). White area on Grande-Terre, flooded Grippon plain graben [see *Feuillet et al.*, 2002] with Mangrove and recent Quaternary clay deposits [e.g., *De Reynal de Saint Michel*, 1966; *Garrabé et al.*, 1988]. (b) Morne-Piton normal fault system with thicker black lines for higher scarps. St. Louis "old" fault in dashed black line (see text). Bathymetry and topography as in Figure 1 (horizontal resolution 50 m) shaded from the south. Contours at 50 m vertical interval. Bathymetry of area contoured with dashed line near Colombie bank and area near the Marie-Galante coast are interpolated with French Service Hydrographique et Océanographique de la Marine available data (notice that SHOM data were not included in the interpolation of the contoured area near Les Saintes).

[10] While it is straightforward to separate and map the three main terraces between la Pointe Des Basses and Ravine Carambole, even where cut into patches, such mapping is difficult farther north, near the fault trace. Here, the terraces are narrower and broken into smaller patches. Nevertheless, we identify four terrace levels on aerial photographs, including T4 (Figure 4a and interpretation Figure 4b). The highest level, represented only by a small, isolated remnant 180 m above the sea level, probably corresponds to T1. The intermediate level (probably T2) is composed of small patches, up to ~250 m long and ~100 m wide. The third level, ~50 m above sea level on average, is an additional small terrace, T3 or Vavon terrace. A multiplication of terrace levels near an active fault, where the uplift rate increases, is often observed [e.g., *Bloom et al.*, 1974; *Armijo et al.*, 1996]. We note that the terrace's

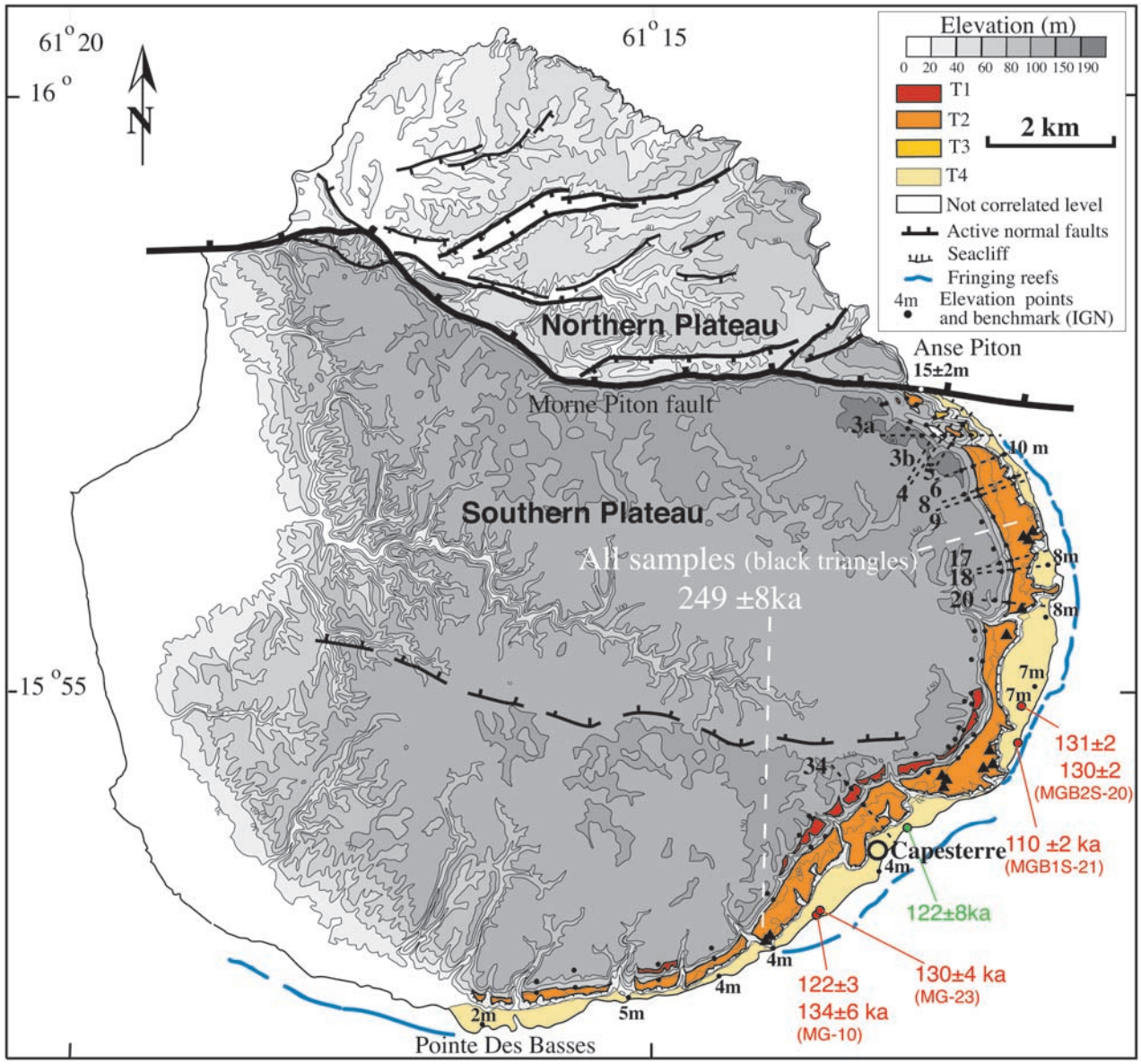

Figure 3. Reef terraces on the Marie-Galante southeastern coast. Topography redrawn from 1/25,000 scale French Institut Géographique National map. Faults as in Figure 2b. In red, orange, dark yellow, and yellow: T1, T2, T3, and T4 terraces, respectively. Upper plateau topography in grey scale. Blue lines, present-day fringing reef. Small black dots, positions of terrace's inner edges and plateau outer edge (see Table 1 and Figure 6). Small white dot with number, elevation of T4 terrace at Anse-Piton from *Feuillet et al.* [2002]. Dashed black lines with numbers, topographic profiles with names shown on Figure 6. Red dots, positions of corals collected on T4 terrace with U/Th ages indicated (see Table 2a). Green dots, position and U/Th age of a coral sampled on T4 terrace by *Battistini et al.* [1986] (see Table 2c). Black triangles, positions of corals sampled on T2 terrace and dated as open systems by *Villemant and Feuillet* [2003] at 249 ± 8 ka (U/Th "model age," see Table 2b).

degradation correlates well with their height and age, T1, which is the oldest, being much more eroded than T4, the youngest.

3. Deformation of the Terraces

3.1. Inner Edges Altitudes and Estimated Uncertainties

[11] To determine the present-day shape of the terraces and of the upper plateau, which are thought to be controlled by slip along the fault, we extracted from the IGN 1/25,000 scale map (precision ±2.5 m), 40 topographic profiles perpendicular to the terraces every 500 m or so. Eleven typical profiles are shown on Figure 6. On each profile, we determined the coordinates (x, y, z) of the inner edge of each terrace, to constrain the altitude and position of the corresponding paleo-sea level [*Lajoie*, 1986]. For the upper plateau, we consider that its seaward edge corresponds roughly to the end of a sea level highstand. The data points

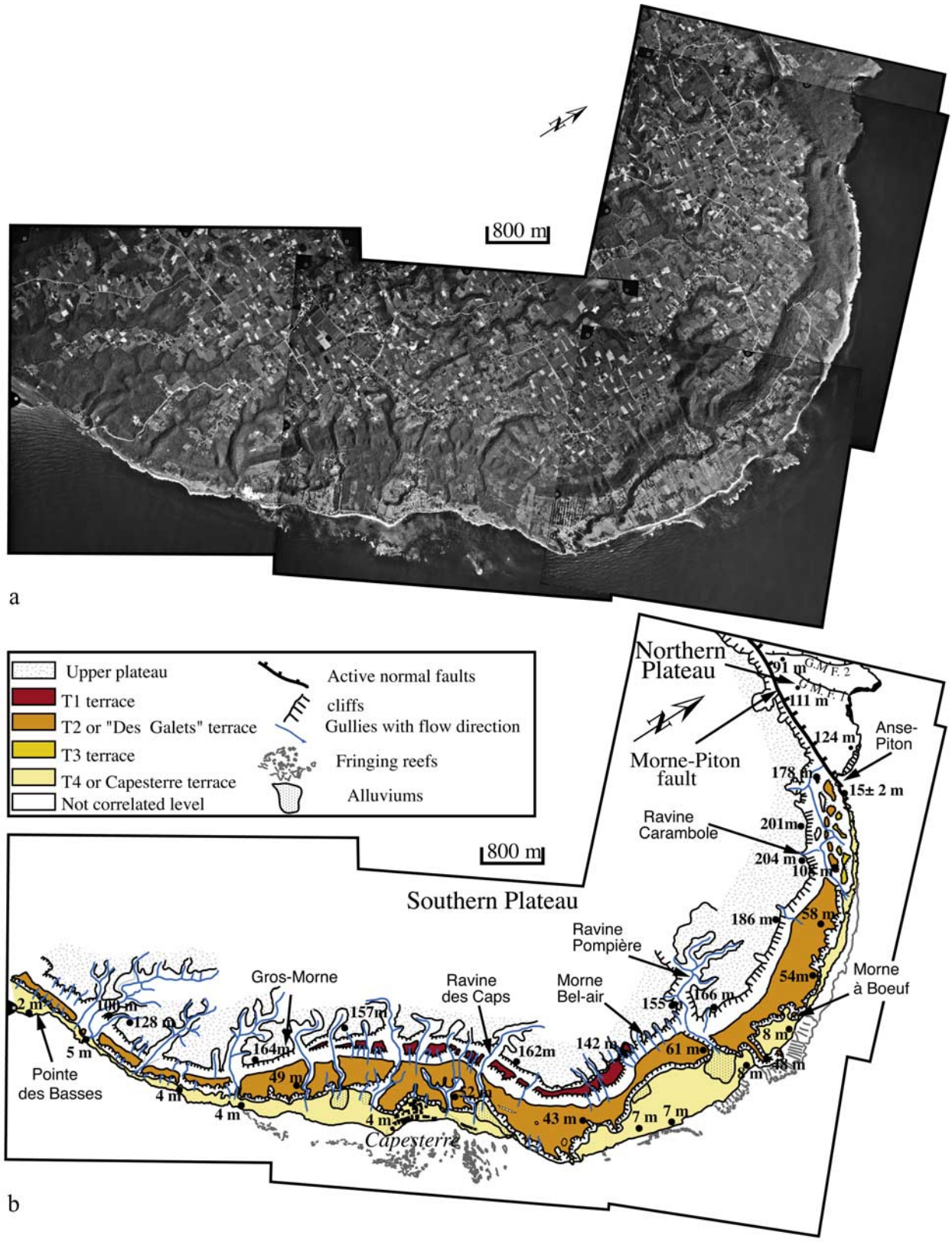

Figure 4. Detailed mapping of Marie-Galante reef terraces on 1:20,000 scale stereoscopic aerial photographs from French Institut Géographique National. (a) Aerial photographs mosaic of the Marie-Galante southeastern coast. (b) Mosaic interpretation and terraces mapping. Terrace's colors as in Figure 3. Present-day fringing reefs in gray. Black dots, IGN benchmarks with elevations indicated. Blue lines with arrows, gullies with flow direction. Active faults as in Figure 2b. GMF, Gros Morne Fault.

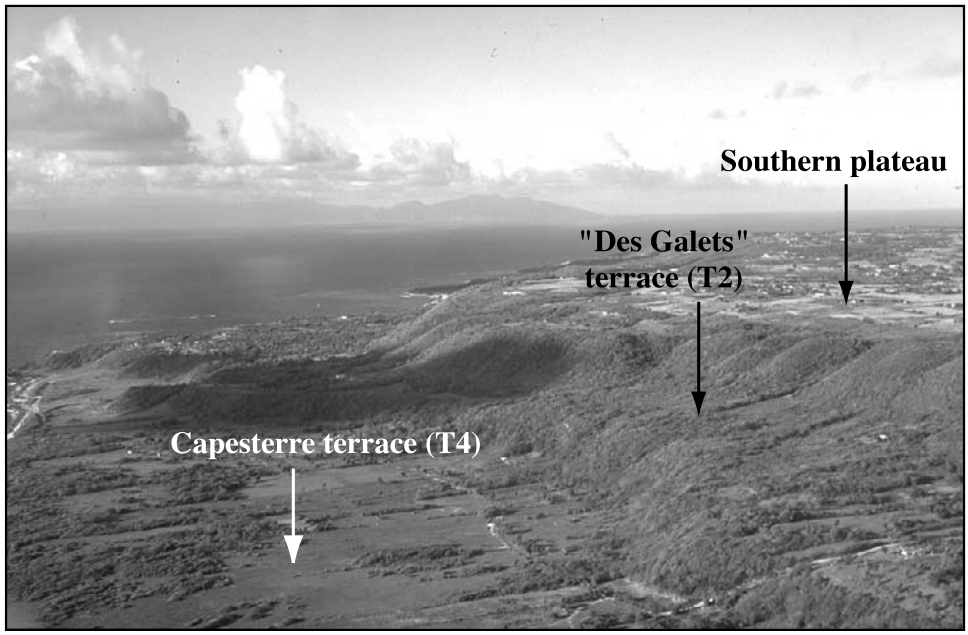

Figure 5. Southward aerial view of the upper reef plateau and of the flight of Quaternary marine reef terraces on Marie-Galante southeastern coast.

are plotted on the map of Figure 3 and listed in Table 1. The altitudes of the terrace inner edges can be overestimated because they are often covered by colluvium (see profiles 6, 8 and 9, Figure 6). Since in general, because of dense vegetation cover, we could not observe the terraces in cross section, the uncertainty on inner edge altitudes is difficult to estimate. Nevertheless we can deduce maximum uncertainties from the profiles. For the T2 terrace, which is up to 700 m wide at places, such altitudes are well constrained by the intersection between its well defined, gently seaward sloping surface and the steepest slope of its relict sea cliff (e.g., profiles 20, 34, Figure 6). North of Ravine Pompière (profiles 6, 8, and 9, Figure 6), the colluvial wedge of the relict sea cliff of T2 has steeper slope, and we infer that the inner edge altitude might be overestimated by up to 10 m. The T1 terrace is narrower and its surface slope constrained by 2 points, at most, on each profile (see profile 34, Figure 6). We consequently assumed T1 to be horizontal with its seaward edge altitude corresponding to that of its inner edge. This hypothesis leads to an underestimation of the inner edge elevation by 10 m at most. The T4 inner edge is covered by alluvium deposited by the principal gullies. Moreover, the map resolution does not allow a determination of its inner edge altitude. We thus also approximated T4 by a horizontal surface, as observed in section along the southeastern coast of Marie-Galante (Petite Anse) and at Anse-Laborde in Grande-Terre by *Battistini et al.* [1986] (see location on Figure 2a). The topographic benchmarks located on this terrace, near the coast, are thus taken to indicate the inner edge altitude (Figure 3 and Table 1). At Anse Piton, the altitude of T4 was estimated to be 15 ± 2 m [*Feuillet et al.*, 2002]. Given the precision of the topographic map, the uncertainty on the upper plateau's seaward edge elevation is less than 5 m. For the small terrace patches near the Morne-Piton fault, we took the few benchmark elevations available to indicate those of their inner edges (see profiles 3a, 3b, 4, and 5, Figure 6). The uncertainties of inner edges horizontal positions are less than 25 m on the 1/25,000 scale topographic map.

3.2. North-South Deformation of the Terraces

[12] The N-S projection, perpendicular to the fault, of the elevations of the terraces inner edges and of the upper plateau's seaward edge shows that all the surfaces are tilted southward (Figure 7a). Their shapes suggest footwall flexure associated with normal slip on the Morne-Piton fault. Away from the fault, the upper plateau elevation decreases progressively from 204 ± 2.5 to 140 ± 2.5 m (−64 ± 2.5 m) over a distance of ∼8.5 km. Note that the upper plateau profile is also disrupted where it crosses the "old" St Louis fault [*Feuillet et al.*, 2002]. By contrast, the T2 elevation profile is continuous, which implies that the St Louis fault stopped moving before the abandonment of T2. Three points close to the fault, corresponding to the inner edge of small, intermediate terrace level patches north of Ravine Carambole, reach elevations of 105−108 + 12.5/−2.5 m. If this level is interpreted to correspond to T2, then the elevation of T2 decreases by 68 + 12.5/−2.5 m southward, away from the Morne Piton fault, over a distance of ∼8.5 km. If these points are left out, the elevation decrease is only 45 + 2.5/−12.5 m. If we infer that the isolated 178 m high patch observed north of Ravine Carambole, above T2, corresponds to a terrace level identical with T1, then the altitude of T1 decreases southward by about 48 + 12.5/−2.5 m, over a distance of ∼6.5 km. Unfortunately, T1 is too small and discontinuous for its shape to be constrained precisely. The elevation of T4 decreases southward, away from the fault by 13 ± 2 m over a distance of 8.5 km.

[13] As generally observed along tectonically rising coastlines around the world [*Lajoie*, 1986], the older terraces are more uplifted and tilted than the youngest, with average regional slopes of 0.45°, 0.3° and 0.07°, for the

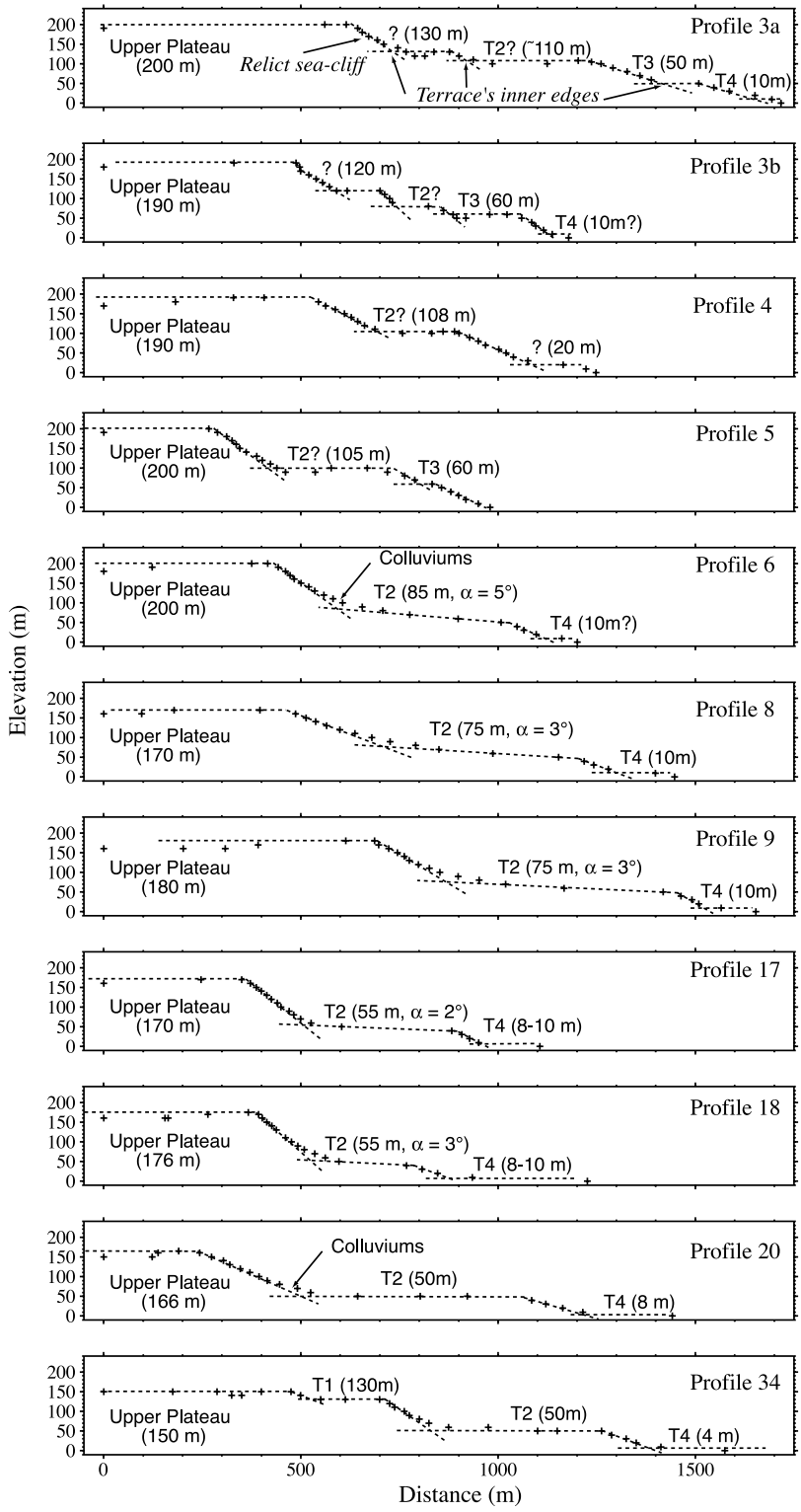

Figure 6. Eleven typical topographic profiles across the Marie-Galante terraces flight and interpretation (dashed line). Profiles locations on Figure 3. The position of terrace inner edge, which approximates a paleo-sea level, is determined by the intersection between the gently seaward sloping terrace and its relict sea cliff [*Lajoie*, 1986]. The altitude of the inner edge can be overestimated by ~10 m when terraces are covered by colluvium (see profiles 6, 8, and 9). Names of terraces with the elevation of their inner edges indicated. Slopes are indicated in degrees.

Table 1. Elevations of Terrace Inner Edges and Southern Plateau Outer Edge on Marie-Galante[a]

Upper Plateau			T1			T2			T3			T4			Not Correlated Level		
x, m	*y*, m	*z*, m	*x*, m	*y*, m	*z*, m	*x*, m	*y*, m	*z*, m	*x*, m	*y*, m	*z*, m	*x*, m	*y*, m	*z*, m	*x*, m	*y*, m	*z*, m
1781	−967	190	1846	−948	**178**	2154	−875	90	2675	−1184	60	2375	−725	15 ± 2	2577	−1438	120
2169	−1334	190	3075	−5150	140	2307	−970	90	3050	−1252	60	3658	−1724	10	2210	−1229	130
2367	−1406	**201**	3019	−5580	130	2455	−1278	**108**	3250	−1412	60	3850	−2075	10			
3004	−1975	200	2995	−5923	130	2729	−1425	105				4343	−3413	**8**			
3048	−2340	170	1407	−6884	130	2852	−1570	**108**				4322	−4224	**8**			
3110	−2418	180	787	−7300	130	3188	−1915	85				4163	−5280	**7**			
3326	−2761	180				3281	−2250	75				3926	−5603	**7**			
3507	−3182	180				3275	−2360	75				1525	−8150	**4**			
3700	−3425	170				3481	−2700	70				200	−9400	**4**			
3658	−3525	**176**				3721	−3117	55				−650	−9825	**4**			
3587	−3950	**166**				3850	−3375	55				−656	−9798	**4**			
3206	−4445	150				3781	−3500	55				−2000	−10175	**5**			
3159	−4884	140				3750	−3975	50				−4287	−10553	**2**			
2900	−5908	150				3369	−4443	65									
2976	−6102	150				3324	−4903	60									
2841	−6211	160				3500	−5600	50									
2343	−6353	160				3216	−6023	55									
1316	−6778	150				3125	−6215	55									
764	−7283	150				2990	−6388	55									
581	−7613	150				2566	−6635	60									
87	−8496	150				1550	−7125	50									
−769	−9350	140				1022	−7652	50									
−1582	−9663	120				783	−7876	50									
−2891	−9608	120				194	−8609	55									
−3455	−9877	100				−693	−9538	40									
2960	−5555	150				−1580	−9900	40									
						−2856	−10063	30									
						−3457	−10074	40									

[a]Origin of coordinates (*x*, *y*) are 689, 1766 (km UTM). Average horizontal and vertical uncertainties on point's positions are ±25 m and ±2.5 m, respectively, on the 1/25,000 scale topographic map of French Institut Géographique National (contours at 10 m interval with few intermediate contours at 5 m interval). Maximum uncertainties on terrace's inner edges altitudes are +10 or −10 m (see text and Figure 6). Institut Géographique National benchmark elevations are indicated in bold.

upper plateau, T2 and T4, respectively. At a more detailed level, there is a hint that T2 and T4 have concave upward profiles, with increasing tilt near the trace of the fault.

3.3. East-West Deformation of the Terraces

[14] On Figure 7b, we projected the elevations of the terraces and plateau edges on an E-W direction. In this direction, which is roughly perpendicular to the arc, all the surfaces are also tilted westward as previously noted on Marie-Galante and Grande-Terre [e.g., *Lasserre*, 1961; *Bouysse and Garrabé*, 1984; *Battistini et al.*, 1986; *Grellet and Sauret*, 1988]. The upper plateau, which is the oldest surface, is more tilted (0.6°) than T2 (0.3°). In turn, T2 is more tilted than T4 (0.08°), which is the youngest terrace. This implies that all the surfaces have been progressively tilted with time. The T2 terrace also becomes progressively narrower and lower, south of Capesterre, to finally disappear at Pointe des Basses.

4. U/Th Ages and Correlation With Paleo-Sea Levels

[15] To estimate the rates of uplift and tilt, we dated different reef terraces and units on Marie-Galante, La Désirade, and Grande-Terre. We collected, according to usual practice [e.g., *Bloom et al.*, 1974], two main species of shallow water coral (Acropora Palmata and Porites) exposed on each well-defined surface (see locations of samples on Figures 2a and 3). Carbonate sediments were also retrieved with a portable coring machine. Thorium and Uranium compositions of the samples were determined at the Géochimie des Systèmes Volcaniques laboratory (Université Pierre et Marie-Curie, Institut de Physique du Globe de Paris, France). The ^{238}U-^{234}U-^{230}Th dating method generally leads to reliable and accurate ages for young corals but to large uncertainties for corals older than 150–200 ka because of diagenesis processes [e.g., *Bard et al.*, 1991, 1990; *Ku et al.*, 1990; *Edwards et al.*, 1987; *Broecker et al.*, 1968]. We date the older altered corals and sediment collected on Marie-Galante terraces using open system evolution models, which allow, in some cases, to pass beyond these problems and to calculate model ages for series of cogenetic carbonates [e.g., *Hendersen and Slowey*, 2000; *Villemant and Feuillet*, 2003, hereinafter referred as VF]. The method is discussed in detail by VF, and the ^{238}U-^{234}U-^{230}Th dating results are presented in Tables 2a and 2b.

[16] The corals sampled on the lowest Marie-Galante terrace (T4) yield individual ages that range between 110 ± 2 and 134 ± 6 ka, with a mean value of 126.2 ± 3 ka (Table 2a). These ages are consistent both with the VF "model age" of 125 ± 5 ka (Table 2b) and with the U/Th 122 ± 8 ka age [*Battistini et al.*, 1986] previously obtained for the same terrace level (Table 2c). On Grande-Terre and La Désirade, the U/Th dating of corals (D4-96B, GTM33-b) sampled on the lowest terraces yield ages of 150 ± 3 and 141 ± 7 ka, respectively (Table 2a). The oldest age we obtained (277 ± 11 ka) is for the polyp unit sampled on the upper plateau of Grande-Terre (GTH 47, Table 2a). The U/Th open system dating method also yields an old age

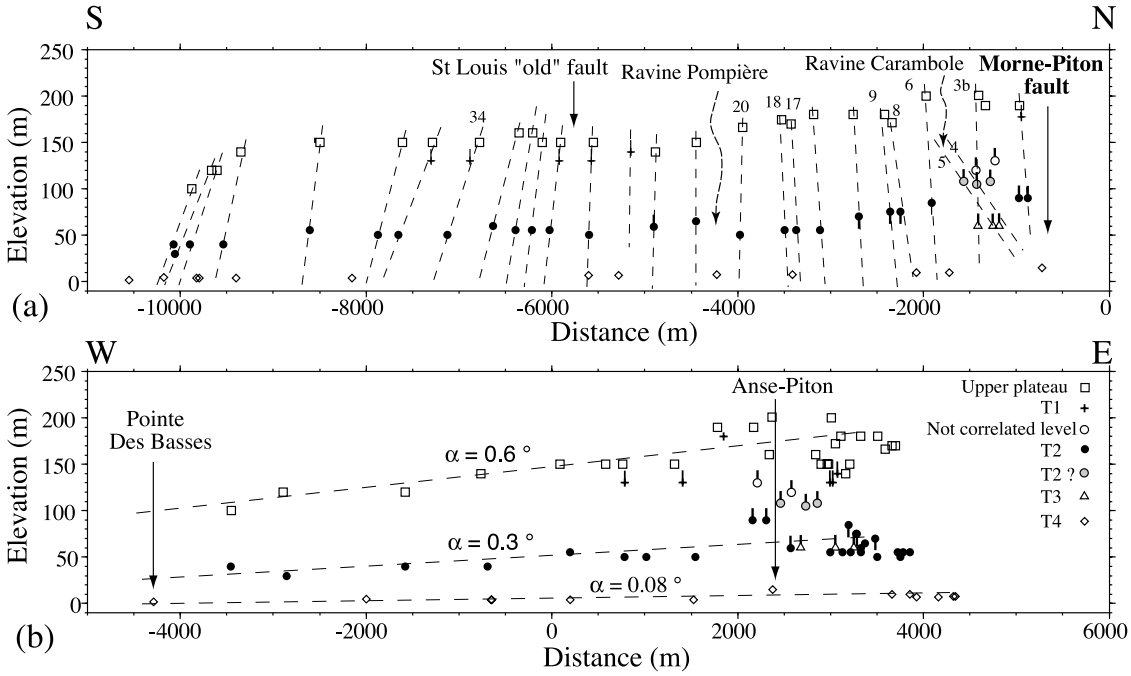

Figure 7. Marie-Galante terraces and upper plateau deformation. Vertical exaggeration 10. (a) Projection in a N-S direction (perpendicular to the Morne-Piton fault) of terrace's inner edges and upper plateau outer edge altitudes determined on topographic profiles (see profiles on Figure 6, point's positions on Figure 3 and coordinates in Table 1). White squares, upper plateau; black crosses, T1 terrace; white dots, not correlated level; black dots, T2 terrace; gray dots, T2 or other level; white triangles, T3 terrace; white lozenges, T4 terrace. Dashed lines, projected profiles. The profiles shown in Figure 6 are numbered (location of the profiles on Figure 3). North of Ravine Carambole, we do not project all profiles for clarity. Symbol sizes are, in general, slightly greater than errors on point's positions (see text and Table 1) except for few points for which the vertical position can be overestimated by up to 10 m, due to presence of colluviums, or underestimated by 10 m, at most, when the terraces are inferred to be horizontal (see text). (b) Projection in an E-W direction of terrace's inner edges and upper plateau outer edge altitudes determined on topographic profiles. Symbols and errors as in Figure 7a. The elevation profiles show that the upper plateau and terrace are tilted to the west. The profiles converge, with the older level (upper plateau) more tilted (0.6°) than the T2 terrace (0.3°), itself more tilted than the youngest terraces T4 (0.08°).

(249 ± 8 ka) for T2 on Marie-Galante (VF date, Table 2b). Unfortunately, the highest terraces and upper plateaus on either Marie-Galante, La Désirade, or northern Grande-Terre could not be dated with either isochron methods.

[17] The age ranges obtained are plotted on the SPECMAC $\delta^{18}O$ isotopic curve on Figure 8 [*Imbrie et al.*, 1984]. The age range of the youngest terrace, T4, indicates that it formed during the isotopic stage 5.5, i.e., the penultimate interglacial, a sea level highstand. We infer that the lowest terraces on Grande-Terre and La Désirade are coeval with T4 on Marie-Galante. That the ages obtained (141 ± 7 and 150 ± 3 ka) significantly predate the 125 ka highstand may reflect opening of the U/Th system related to diagenesis processes such as recoil effects or Thorium addition [*Henderson and Slowey*, 2000; *Gallup et al.*, 1994; *Villemant and Feuillet*, 2003]. The "model age" of the T2 terrace (249 ± 8 ka) on Marie-Galante suggests that it formed during the isotopic stage 7.5, also a main sea level highstand.

Table 2a. U/Th Ages of Corals Collected at Marie−Galante, Grande-Terre and La Désirade[a]

Terrace	Sample	Specie	[U], ppm	$^{230}Th/^{234}U$	$^{234}U/^{238}U$	$^{234}U/^{238}U0$	Calcite, %	Altitude, m	Age, ka
T4 (Marie-Galante)	MG-10-A	Acropora	5.7	0.686 ± 0.011	1.120 ± 0.010	1.167 ± 0.014	–	1.5	122 ± 3
T4 (Marie-Galante)	MG-10-B	Acropora	4.9	0.723 ± 0.017	1.113 ± 0.013	1.163 ± 0.019	–	1.5	134 ± 6
T4 (Marie-Galante)	MGB2S-20	Acropora	**4.0**	0.712 ± 0.006	1.113 ± 0.009	1.161 ± 0.012	10.4	7	131 ± 2
T4 (Marie-Galante)	MGB2S-20	Porites	**3.0**	0.705 ± 0.007	1.060 ± 0.011	1.085 ± 0.016	2.8	7	130 ± 2
T4 (Marie-Galante)	MGB1S-21	Acropora	**3.4**	0.648 ± 0.006	1.118 ± 0.009	1.159 ± 0.012	8.9	3–4	110 ± 2
T4 (Marie-Galante)	MG-23	Acropora	5.2	0.711 ± 0.013	1.127 ± 0.012	1.180 ± 0.017	–	3–4	130 ± 4
T4 (La Désirade)	D4-96B	Acropora	2.4	0.740 ± 0.21	1.123 ± 0.026	1.180 ± 0.038	–	5	141 ± 7
T4 (Grande-Terre)	GTM33-b	porites	2.8	0.765 ± 0.009	1.139 ± 0.012	1.209 ± 0.019	0.6	0.5–1	150 ± 3
Upper Plateau (Grande-Terre)	GTH47	porites	2.9	0.942 ± 0.012	1.078 ± 0.014	1.166 ± 0.030	3.1	25	277 ± 11

[a]Uranium concentrations in bold were measured by neutronic activation at CEA-CNRS Pierre Süe Laboratory (Saclay, France). See sample locations on Figure 3.

Table 2b. U/Th "Model Ages" Obtained by *Villemant and Feuillet* [2003] at Marie-Galante

Terrace	Model Age, ka
T4 (Marie-Galante)	125 ± 5
T2 (Marie-Galante)	249 ± 8

[18] Considering that the past interglacial terraces were formed at sea levels that differ by at most few meters from the present-day sea level [e.g., *Armijo et al.*, 1996, and reference therein], the age and average altitude (~50 m) of T2 imply an uplift rate of ~0.2 mm/yr. In general, coastlines that are uplifted at such slow rates record only the most prominent highstands, which correspond to interglacials [e.g., *Armijo et al.*, 1996, and references therein]. In keeping with this simple hypothesis, we infer that the upper plateau of Marie-Galante, which is the only extensive surface above T2, emerged during isotopic stage 9.3 (330 ± 10 ka), soon after the formation, near the sea surface, of the thin polyp unit. Indeed, the fossil sea cliff that bounds the plateau, 100 m high on average, likely marks a main interglacial signal. Note, however, that since the eastern edge of the plateau is on average 150 m above sea level, a 330 ± 10 ka age would imply an average uplift rate of ~0.4 mm/yr, twice as fast than that since 250 ka.

[19] A minimum vertical throw rate of ~0.4 mm/yr is obtained on the Morne-Piton fault using the age of the upper plateau (330 ± 10 ka) and the maximum height (~130 m) of the cumulative scarp. We also constrained the shapes and ages of two terraces south of the fault (T2 and T4). Because they exist only on the fault footwall, however, these surfaces cannot be used directly to determine fault slip. A way to use the latter terrace profiles to further constrain the slip rate is to model the vertical displacements recorded by the terrace.

5. Modeling

[20] To model the growth of topography, we follow the approach pioneered by *King et al.* [1988] and *Stein et al.* [1988], which is based on the assumption that finite deformation results from the sum of many earthquake cycles. They used a thin plate approximation to represent an elastic plate overlying a viscous lower crust. In this approach, reduced strength in the seismogenic crust was represented by an effective elastic thickness which was always less than the seismogenic thickness. *King and Ellis* [1991] modified the approach modeling the seismogenic crust using the known thickness and instead reducing the modulus to represent a loss of crustal strength. *Armijo et al.* [1996] adopted the same approach to model terrace's shapes in Corinth (Greece). For these terraces it was found that when the modulus was reduced sufficiently to fit the data, the vertical displacements predicted by the model at the surface were almost identical to those for a fault with the same geometry in a homogeneous elastic half-space. Hence, on the basis of these results and other studies favoring the half-space approximation [e.g., *Valensise and Ward*, 1991], we consider the Morne-Piton fault segments as planar dislocations in a Poissonian elastic half-space ($\lambda = \mu =$ 32 GPa). The vertical displacements induced at the surface by motion along such dislocations are calculated using *Okada*'s [1985, 1992] equations and vary only as a function of the dislocation geometry (slip, dip, and depth).

[21] The three-dimensional model is shown in Table 3 and in map view with initial and residual topography and in N-S cross section on Figure 9. It reproduces as well as possible the Morne-Piton fault geometry. We also took into account the smaller synthetic and antithetic faults connected to the main one, which accommodate part of the deformation. The motion is dip slip on E-W striking segments (N-S extension), and all segments intersect the surface.

5.1. Model Calibration From Plateau Modeling

[22] To calibrate the model, we first reproduce the shape of three topographic profiles perpendicular to the fault (A, B, and C, in Figure 9a). The three profiles were extracted from the IGN digital elevation model (50 m horizontal resolution) in the western part of Marie-Galante, where the morphology of the plateau, north of the Morne-Piton fault, is smooth and only mildly perturbed by erosion. The vertical throws are deduced from the profiles. We vary only the dip and depth of the main dislocation (Morne-Piton segments, in bold Figure 9a), the geometry of smaller secondary faults remaining unchanged.

[23] The three topographic profiles show that Marie Galante's southern and northern plateaus are flexed upward and downward, respectively, on either side of the Morne-Piton fault, and tilted toward the south, as are the reef terraces (Figure 10). Although the topography of the southern plateau is disrupted by the old St Louis fault scarp, this is not taken into account in the modeling, because that fault is no longer

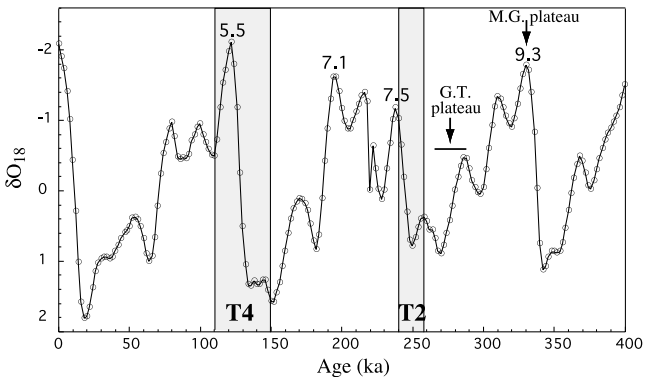

Figure 8. Correlation between terrace's U/Th ages and the SPECMAC orbitally tuned deep-sea oxygen isotope record [*Imbrie et al.*, 1984], with peaks corresponding to interglacials and high sea levels. Gray bars, T2 "model age" [*Villemant and Feuillet*, 2003] (see Table 2b) and T4 age ranges (see Table 2a). Horizontal black line, age of the coral collected on Grande-Terre upper plateau (GTH 47, see Table 2a). Black arrow, Marie-Galante plateau inferred age (see text). G.T., Grande-Terre; M.G., Marie-Galante.

Table 2c. U/Th Ages of Corals Sampled on Grande-Terre, Marie-Galante, and La Désirade Obtained by *Battistini et al.* [1986][a]

Localities	Altitude, m	Calcite, %	Age, ka
Grande-Terre (Anse Laborde)	3	0	158 ± 15
Grande-Terre (Anse Laborde)	3	2	149 ± 11
Marie-Galante (Capesterre)	3.5	0	122 ± 8
Désirade (Pointe des Colibris)	2.5	1	119 ± 9

[a]See locations on Figures 2a and 3.

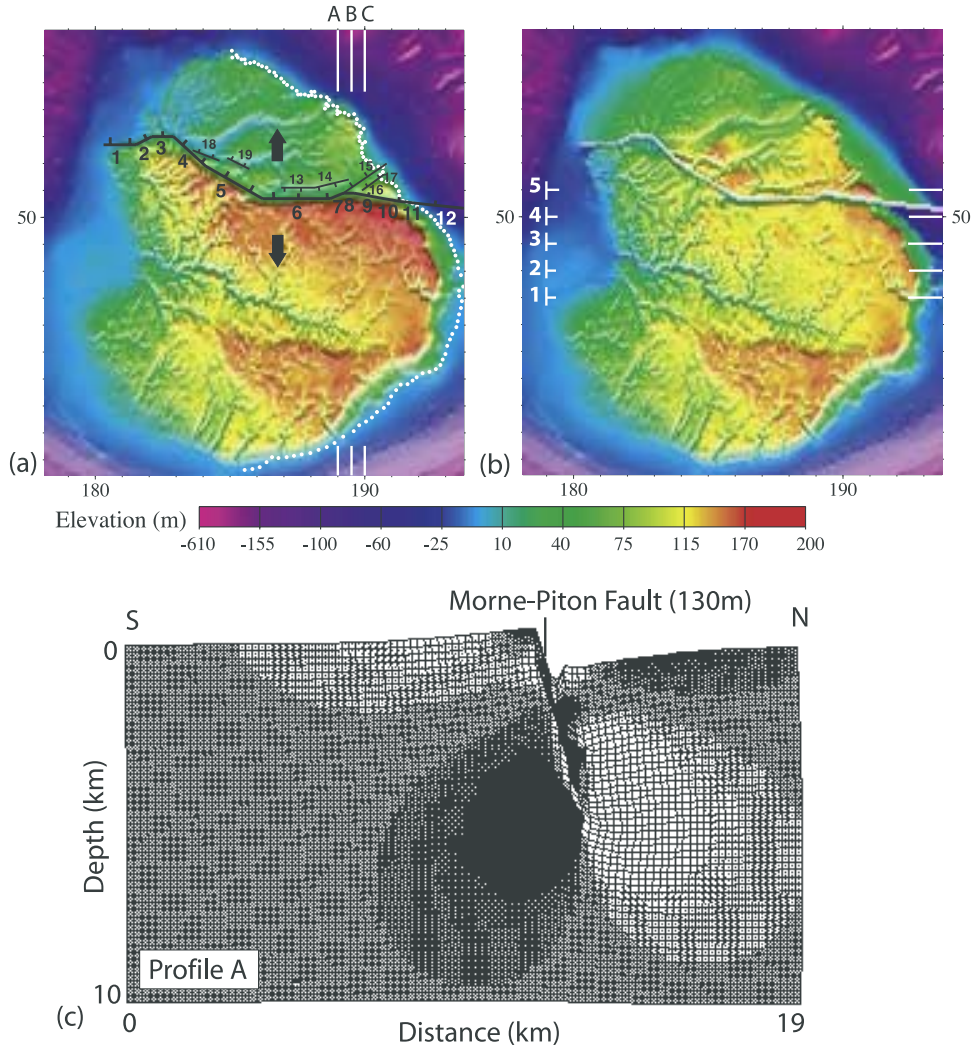

Figure 9. Morne-Piton fault modeling. Topography as in Figure 2b. Coordinates in km Mercator with the reference point at latitude 15°30′N and longitude 63°W. (a) Model in map view with present-day topography. Each fault segment is numbered (see Table 3). The Morne-Piton fault segments are modeled as dislocations (black lines with ticks, with thicker trace for higher slips) in an elastic half-space (see text). Double black arrows, direction of extension. The motion is dip slip on E-W striking faults. White lines with letters (A, B, C), location of topographic profiles shown on Figure 9c (profile A) and 10. White dots along coast, location of profile modeled in Figure 11 (see caption). (b) Residual topography, before motion of the Morne-Piton fault. Notice that the island remains clearly tilted westward. Numbered white lines, residual topographic profiles shown in Figure 13a. (c) Deformation model in section along the profile A (location Figure 9a). Vertical exaggeration 1. Each square is 200 m by 200 m. Dark shading, areas of dilatation; light shading, areas of compression. The main fault (Morne-Piton) is associated with a smaller antithetic fault. Both the footwall and the hanging wall of the main dislocation are flexed and tilted southward as observed for terraces (see text).

active. In any case, its throw is too small (<40 m) to affect significantly the overall flexure of the southern plateau. Figure 10 shows the modeled surface vertical displacements for different dips (60°, 70°, and 80°, Figure 10a) and depths (2.5, 5, and 10 km, Figure 10b) of the main dislocation, the amount of cumulative slip being fixed to correspond to the cumulative throw (100–130 m, see Table 3). The effect of varying faulting depth results in greater differences than changing the dislocation dip. This is particularly clear for the hanging wall profile, which is more flexed with smaller faulting depth. The best fit, determined by trial and error, is obtained with a dislocation depth of 5 km and a dip ranging between 70° and 80°, in agreement with the actual dip of the Morne-Piton fault plane as exposed at Anse-Piton [*Feuillet et al.*, 2002]. A dip of 70° explains better the hanging wall profile. A dip of 80° fits the flexure of the footwall better. Even if karstic and stream erosion on the footwall, probably maximum near the St. Louis river, slightly exaggerated the footwall flexure, a dip of 60° would not fit the shape of the southern plateau.

5.2. Terrace Modeling and Fault Slip Rate

[24] Using the dislocation parameters (dip and depth) deduced from modeling the profiles of the Marie-Galante

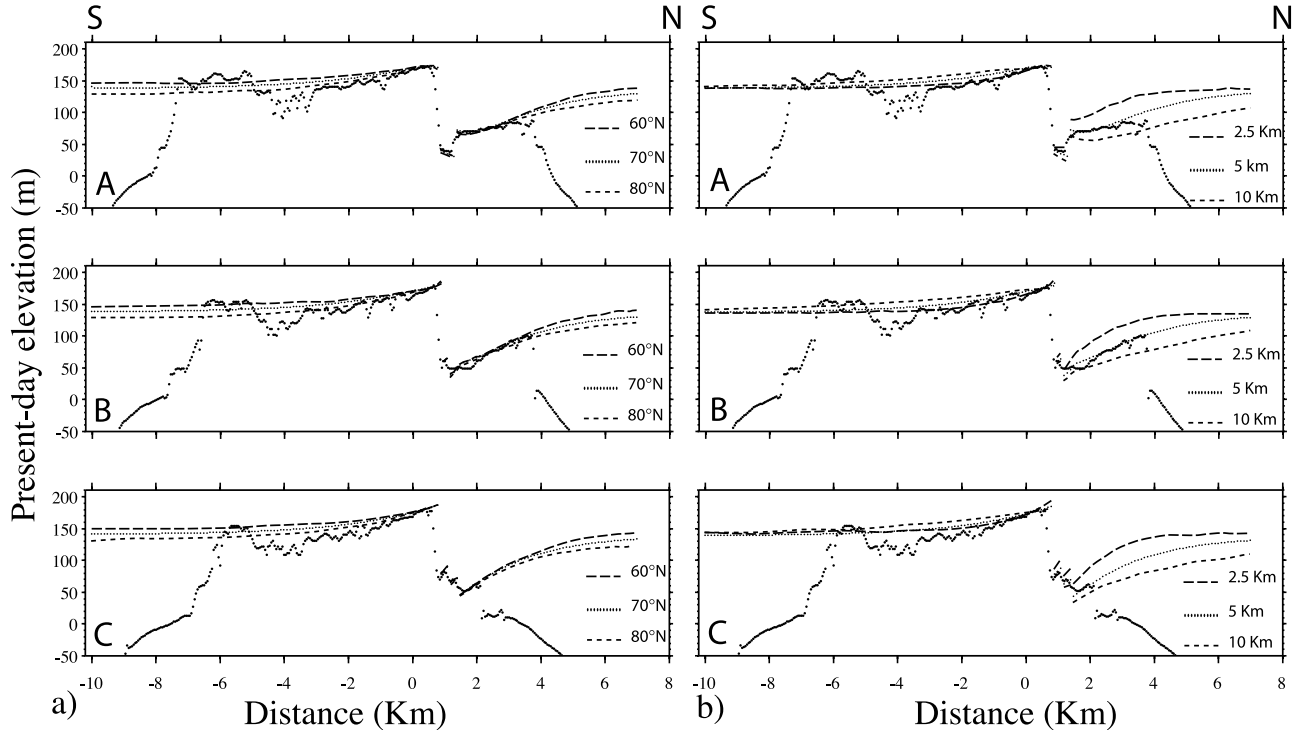

Figure 10. Modeling of upper plateau topographic profiles on Marie-Galante. Location of the three profiles on Figure 9a. Topography from digital elevation model of Figure 9a. Vertical exaggeration 20. Distance in km from latitude 50 km on Figures 9a and 9b. Dotted and dashed curves, modeled vertical displacements. Notice that the curves are shifted upward by ~150 m to be compared to the present-day topography of the plateau, the modeled vertical displacements being quasi-null, tens kilometers far from the dislocation. (a) Changing fault dip between 60 and 80°, depth (width in Table 3) and slip being fixed. (b) Changing fault depth between 2.5 and 10 km, dip and slip being fixed.

plateau, we now turn to fit the terraces and upper plateau shapes along the island eastern coast by changing the amounts of cumulative slip as a function of age (Figure 11). Only the results for a dip of 80° are shown, since the terraces are on the footwall. To fit the shape of the upper plateau, along the coastline, the cumulative slip on the main fault and on adjacent faults dislocations must be increased by 20%. Greater throws thus exist at Anse-Piton, where stream incision precludes a precise estimate of the Morne-Piton scarp height. The total slip ranges between 235 and

Table 3. Upper Plateau Calibrated Model and Dislocation Parameters[a]

Dislocation	Longitude, km	Latitude, km	Strike, deg	Dip, deg	Length, km	Width, km	Rake 1, deg	Slip 1, m	Rake 2, deg	Slip 2, m
1	180.9	52.7	90	80°N	1.2	5	90	50	90	53
2	181.8	52.85	63.5	80°N	0.7	5	85	112	80.3	118
3	182.5	53.0	90	80°N	0.8	5	90	112	90	117
4	183.5	52.45	132.5	80°N	1.6	5	−81	134	−72.5	144
5	185.15	51.3	120	80°N	2.4	5	−84	133	−78.9	140
6	187.45	50.7	90	80°N	2.5	5	90	132	90	138
7	188.95	50.8	68	80°N	0.54	5	86	132	82.2	139
8	189.4	50.9	90	80°N	0.4	5	90	132	90	138
9	190.15	50.8	100.4	80°N	1.12	5	−88.2	112	−87.2	117
10	191.0	50.65	99	80°N	0.6	5	−88.3	132	−87.2	138
11	191.75	50.55	96.3	80°N	0.9	5	−88.9	132	−87.8	138
12	193.6	50.35	96.0	80°N	2.8	5	−88.9	132	−87.2	138
13	188.52	51.1	90	90°	1.24	1	90	42		
14	188.77	51.25	76.5	90°	1.28	1	89.8	40	–	–
15	190	51.45	55.5	70°N	1.94	2.5	77.1	32	–	–
16	190.05	51.12	52.5	70°N	0.38	2.5	75.6	32	–	–
17	190.45	51.41	52.5	70°N	0.62	2.5	75.6	32	–	–
18	185.3	52.0	116.6	70°N	0.9	2.5	−80.3	75	–	–
19	184.1	52.3	112	70°N	1.08	2.5	−82	75	–	–

[a]See locations on Figure 9a. Coordinates are in kilometers Mercator with the reference point at 15°30′N of latitude and 63°W of Longitude. Negative and positive rakes are for left- and right-lateral component of motion, respectively. Rake 1, slip 1 are for a dip of the main dislocation (Morne-Piton) of 80°N. Rake 2, slip 2 are for a dip of the main dislocation of 70°N.

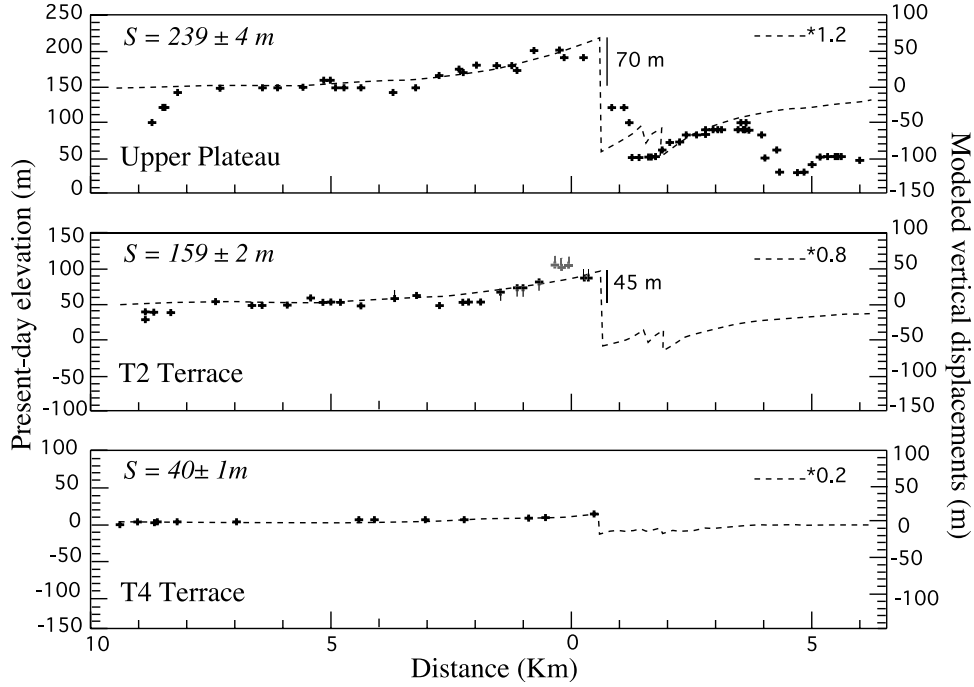

Figure 11. Modeling upper plateau and T2 and T4 terrace's shape along the coast (see white dots on Figure 9a). Vertical exaggeration ~15. Distance in km as in Figure 10. Dashed curves, modeled vertical displacements; *1.2, *0.8, and *0.2 indicate that slips of "plateau-calibrated" model (see Table 3) are multiplied by 1.2, 0.8, and 0.2 to fit the surface's shapes. Crosses, terrace's inner edges and upper plateau elevations (see Table 1). Numbers in italic, total cumulated slip (in m) on dislocations (Morne-Piton and Gros-Morne smaller synthetic faults, see map on Figure 3 and model on Figure 9a). Vertical bars with numbers, maximum cumulative footwall uplift deduced from modeling.

243 m, depending on fault dip. This takes into account secondary faults (Gros-Morne) that merge laterally with the main fault and likely also do so at depth.

[25] To fit the T2 terrace shape, we need a total slip of 159 ± 2 m (0.8* plateau-calibrated model) or 239 ± 4 m (1.2* plateau-calibrated model), depending on whether the 105 − 108 + 12.5/−2.5 m high points south of the main fault are included or not. Since it is unlikely that the shape of the T2 terrace, which is likely ~100 ka younger than the upper plateau, results from the same amount of slip, and since the corresponding model does not provide a good fit to other points at elevations ≥60 m located closer to the fault, we conclude that the 105 − 108 + 12.5/−2.5 m high points north of Ravine Carambole do not belong to the T2 terrace. Our preferred model is thus that corresponding to a cumulative slip of 159 ± 2 m. The youngest T4 terrace shape is best fit with a cumulative slip of 40 ± 1 m (0.2* plateau-calibrated model).

[26] The forward modeling results and the ages determined for the upper plateau and the terraces T2 and T4 indicate that the slip rate on the Morne-Piton fault system ranged between 0.7 and 0.3 mm/yr in the last 330 ± 10 kyr, with an average value of 0.5 ± 0.2 mm/yr (Figure 12a). At a more detailed level, motion on the fault may have been faster, by a factor of ~3, prior to ~120 ka (~1.0 mm/yr) than since. Such values are on the low side of those measured on most other normal faults in the world (Afar, Italy, Tibet, 0.7–3 mm/yr [e.g., *Manighetti et al.*, 1998; *Jacques et al.*, 2001; *Armijo et al.*, 1986]). The footwall uplift rate is proportional to the fault slip rate, with a mean value of ~0.15 ± 0.05 mm/yr (Figure 12b).

6. Trench Perpendicular Tilt of Guadeloupe Islands

[27] By subtracting the modeled vertical displacements from the present-day topography, it is possible to retrieve the shape of Marie-Galante before the formation of the Morne-Piton fault (Figure 9b). E-W trending topographic profiles (Figure 13a, see location in Figure 9b), extracted from the digital elevation model (DEM) corrected in this way, show that the plateau remains tilted westward by ~0.35°. Clearly, this residual tilt is unrelated to movement on the ~E-W trending Morne-Piton fault. An E-W topographic profile across the northern plateaus of Grande-Terre, where not cut by large normal faults [*Feuillet et al.*, 2002], shows that it is also tilted westward by ~0.35° (Figure 13d). Its polyp upper unit continues beneath volcano-clastic deposits on the east side of Basse-Terre (Figures 2a, 13b and 13c): it has been found in borehole, at a depth of 70 m below sea level [*Garrabé and Paulin*, 1984]. The Désirade island upper plateau, 10 km east of the eastern tip of Grande-Terre (Pointe Des Chateaux), closest to the trench, is the highest of the archipelago (276 m). When projected perpendicularly to the trench, the two latter points (−70 and 276 m) fit with a regional, 0.35° westward tilt of the surface of all the oldest reef tables capping the eastern islands of the Guadeloupe archipelago (Figure 13c). This suggests that all

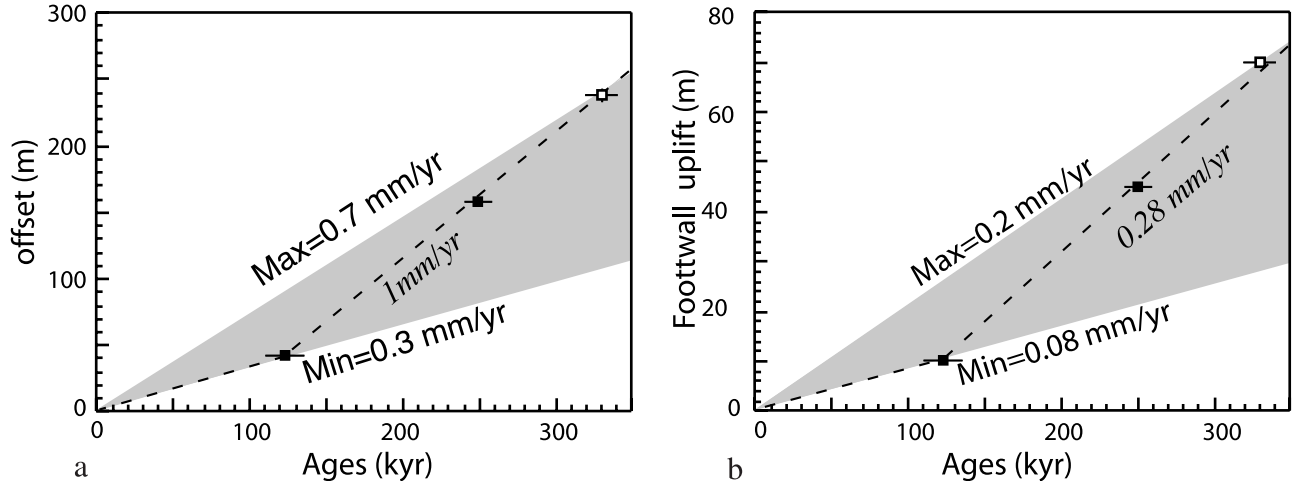

Figure 12. (a) Plot of cumulative offsets on Morne-Piton fault system determined from modeling (italic numbers in meters on Figure 11) as a function of terraces and upper plateau ages. Black squares, terraces dated by U/Th method. White squares, age inferred by correlation with sea level highstands (upper plateau). Bars indicate the uncertainties; 0.3 mm/yr is the lower bound of slip rate constrained by T4 terrace modeling and U/Th age; 0.7 mm/yr is the upper bound constrained by the upper plateau modeling and inferred age. Dashed line, probable evolution of the fault slip rate (1 mm/yr between 330 ± 10 and 120 ± 10 ka, almost 3 times faster than since 120 ± 10 ka). (b) Plot of cumulative maximum footwall uplifts determined from modeling (see Figure 11) as a function of terraces and upper plateau ages. Uncertainties are as in Figure 12a; 0.08 mm/yr is the lower bound of uplift rate constrained by T4 terrace modeling and U/Th age; 0.2 mm/yr is the upper bound constrained by the upper plateau modeling and inferred age. Dashed line, probable evolution of the footwall uplift rate.

these ancient reef platforms emerged at the same time (∼330 ka) and were subsequently tilted uniformly westward, away from the trench, by processes unrelated to arc parallel extension but linked with subduction (Figure 2a).

[28] Such east-to-west tilt is also clear in the present-day morphology of the islands (Figure 2a). The eastern coasts of Grande-Terre and Marie-Galante exhibit steep high cliffs, whereas their low and flat western coasts tend to submerged, with mangrove, and with 6–20 m thick peat in Grande-Terre [*Assor and Julius*, 1983; *Besson and Hamm*, 1983] (Figure 2a). Westward tilting, still active today, has thus increasingly affected all the reef platforms (plateaus and terraces), including the youngest terrace T4 (Figure 13b), and the fringing reefs that are found mostly along the eastern coasts of the islands. The T4 terrace is fairly continuous along the eastern coasts of Grande-Terre and Marie-Galante, with an average altitude of 5–6 m, whereas only isolated small patches, standing just 2–3 m above sea level, remain along the western shores of the two islands [*Battistini et al.*, 1986]. *Grellet and Sauret* [1988] suggested, on the basis of a morphological study made by *Guilcher and Marec* [1978], that the submarine reef platform in the "Grand-Cul de Sac," which is at most 5m deep, corresponds to a submerged equivalent of T4 (Figure 2a). If this inference is correct, the altitude of T4 increased by ∼15 m between the Grand-Cul de Sac and the eastern tip of La Désirade, where it stands 10 m above sea level [*Battistini et al.*, 1986] in the last 125 kyr. The hypothesis that regional tilting started around 330 ka suggests an uplift rate related to subduction of 0.8 mm/yr since that time at La Désirade. Though such tilting continues today, it cannot continue at the same rate, unless T4 has been grossly misidentified at the eastern tip of La Désirade. If the age of the latter terrace is indeed ∼125 ka, then the average uplift rate of La Désirade's eastern prong has only been 0.08 mm/yr since that time.

[29] The eastern plateaus of Grande-Terre, located at roughly the same distance from the trench as Marie-Galante are less uplifted. Their altitude is comparable to that of terrace T2 on Marie-Galante (50 m above sea level, on average). This is consistent with the idea that the two surfaces underwent the same deformation and formed at the same time (∼250 ka, Figure 2a). The age of the coral sampled on the eastern plateau, near Pointe Tarare (277 ± 12 ka), which is ∼30 kyr older than that determined for T2, probably due to diagenesis, supports such coevality (Table 2a and location on Figure 2a). That the eastern plateaus are younger than the northern plateau of Grande-Terre is compatible with the fact that the cumulative throws on the faults that cut the northern plateau are the largest of the island [*Feuillet et al.*, 2002].

7. Summary and Implications for Seismic Hazard

[30] The reef plateau and terraces of Marie-Galante have undergone two deformation episodes of different origin: a local deformation related to normal downthrow along the Morne-Piton fault, and a westward regional tilt that affects all the Guadeloupe islands, likely related to subduction.

[31] Normal slip on the E-W trending, active Morne-Piton fault, the largest of the archipelago, has been taking place at an average rate of ∼0.5 ± 0.2 mm/yr in the last 350 kyr. The vertical offsets of Marie-Galante's upper plateau and of the two main marine terraces along its eastern coast further suggest that the slip rate has decreased from a maximum of ∼1 mm/yr prior to ∼120 ka to a slower value (∼0.3 mm/y)

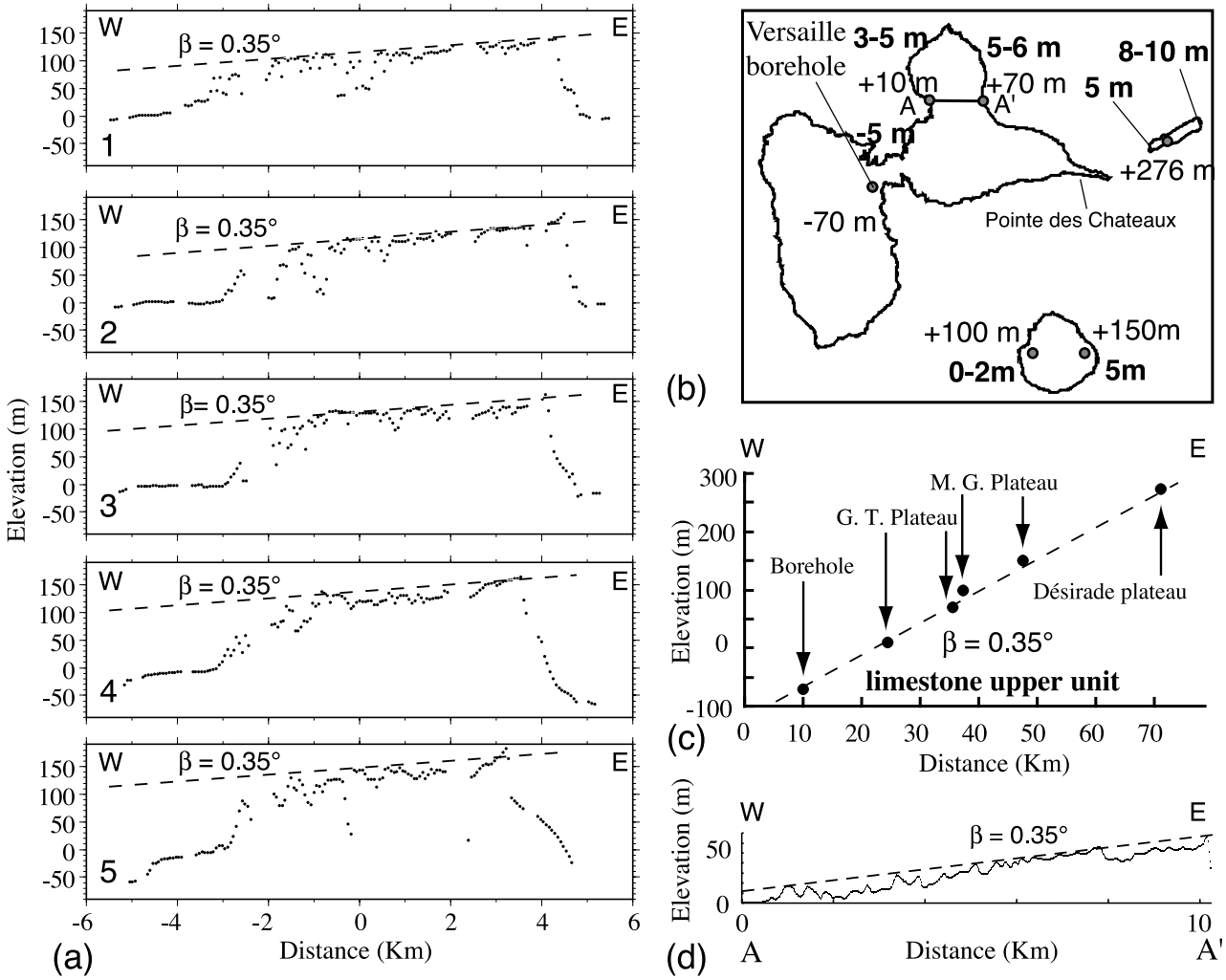

Figure 13. Westward tilting of Guadeloupe archipelago. (a) W-E profile from residual Digital elevation model (Figure 9b). Dashed lines indicate westward tilting by 0.35° of the Marie-Galante island. (b) Reef plateaus of Guadeloupe archipelago with elevation in meters (gray dots with numbers, see text). On Marie-Galante, the elevations are corrected from the local deformation due to normal faulting (see Figures 9b and 13a). Bold numbers, elevation of T4 terrace in the whole archipelago from *Battistini et al.* [1986]. Location of topographic profile AA′ (Figure 13d) on Grande-Terre is indicated. (c) Trench perpendicular projection (i.e., in a N80°E direction) of the Guadeloupe reef plateaus (limestone upper unit) altitude (gray dots of Figure 13b) with whole tilt indicated in degrees. (d) W-E topographic profile (A-A′) of Grande-Terre northern plateau (see location on Figure 13b).

since that time. Knowing the slip rate and the geometry of the Morne-Piton fault, we can draw inferences on earthquake size and place bounds on earthquake recurrence time on this fault. The total length of the Morne-Piton fault system is ~50 km. It is divided into five main segments, 5 to 15 km long. If the entire fault system ruptured during one single earthquake, the ruptured area would reach a maximum of 250 km^2. Using the empirical relation of *Wells and Coppersmith* [1994]: $M_w = 4.07 + 0.98 \log a$, one would obtain a maximum moment magnitude of 6.5. Kanamori's relationship ($M_w = (2/3)\log(\mu S \Delta u) - 6.03$) [*Kanamori*, 1977] would imply ~1 m of slip for such an event and an average recurrence time ranging between 1400 and 3300 years, given the upper (0.7 mm/yr) and lower (0.3 mm/yr) bounds determined for the slip rate. No earthquake of such magnitude has been reported in the historical catalogue since 1530 [*Robson*, 1964]. In any case, the longest recurrence time is more likely since the present-day slip rate appears to be close to the lower bound. A more plausible assumption is that only shorter segments of the Morne-Piton fault system rupture during single earthquakes. Historically, such earthquakes have been recorded (Figure 1). If, for instance, only the 15 km long segment that crosses Marie-Galante ruptured in a single event, this event would have a M_w magnitude = 5.8, comparable to that of the 5 January 2001 earthquake (Figure 1), with a slip of 0.3 m, and a recurrence time ranging between 400 and 1000 years.

[32] The westward tilt of the Guadeloupe archipelago's most ancient reef platform is observed at distances ranging between 80 and 140 km from the Caribbean trench (see

Figure 1, inset). As observed along many subduction zones (e.g., Japan [e.g., *Thatcher*, 1984] and SW Pacific [e.g., *Taylor et al.*, 1987]), such tilt, and the corresponding variable uplift, are probably a consequence of deformation at the subduction interface. Though modeling of this deformation is beyond the scope of this paper, the long-term vertical displacements observed in Guadeloupe broadly resemble the coseismic displacements that would result from megathrust earthquakes. Since they reflect significant buildup of topography, however, and since the 330 and 250 ka rates of uplift and tilt appear to have been ten times larger than present-day rates, the corresponding subduction interface deformation cannot have been steady state. It may correspond to transient underthrusting of an asperity of the Atlantic seafloor, and/or a growth episode of the accretionary prism.

[33] **Acknowledgments.** We thank French Institut National des Sciences de l'Univers, French Centre National de la Recherche Scientifique (programme PNRN), and Institut de Physique du Globe de Paris for financial support. We are grateful to G. Boudon, the late J. C. Rossignol, and the staff of Observatoire Volcanologique de la Soufrière for assistance in the field. We thank the late P. Ildefonse for X-ray measurements on coral samples. We thank R. Armijo and B. Meyer for helpful discussions. We are grateful to the Associate Editor J. Braun and an anonymous referee for constructive reviews. This is IPGP contribution 1935.

References

Andreieff, P., P. Bouysse, and D. Westercamp (1989), Géologie de l'arc insulaire des Petites Antilles et évolution géodynamique de l'Est-Caraïbe, *Doc. B. R. G. M.*, *171*, 385 pp.

Armijo, R., P. Tapponnier, J. L. Mercier, and H. Tonglin (1986), Quaternary extension in southern Tibet: Field observations and tectonic implication, *J. Geophys. Res.*, *91*, 13,803–13,872.

Armijo, R., B. Meyer, G. C. P. King, A. Rigo, and D. Papanastassiou (1996), Quaternary evolution of the Corinth Rift and its implications for the Late Cenozoic evolution of the Aegean, *Geophys. J. Int.*, *126*, 11–53.

Assor, R., and C. Julius (1983), Caractéristiques sédimentologiques et micropaléontologiques de la lagune de Belle Plaine (mangrove de Guadeloupe), *Bull. Soc. Geol. Fr.*, *25*, 889–902.

Bard, E., B. Hamelin, R. G. Fairbanks, and G. Richard (1990), U-Th ages obtained by mass spectrometry in corals from Barbados; sea level during the past 130,000 years, *Nature*, *346*, 456–458.

Bard, E., R. G. Fairbank, B. Hamelin, A. Zindler, and C. T. Hoang (1991), Uranium-234 anomalies in coral older than 150,000 yrs, *Geochim. Cosmochim. Acta*, *55*, 2385–2390.

Battistini, R., F. Hinschberger, C. T. Hoang, and M. Petit (1986), La basse Terrasse corallienne (Eémien) de la Guadeloupe: Morphologie, datation $^{230}Th/^{234}U$, néotectonique, *Rev. Géomorph. Dyn.*, *35*, 1–10.

Bernard, P., and J. Lambert (1988), Subduction and seismic hazard in the northern Lesser Antilles arc: Revision of the historical seismicity, *Bull. Seismol. Soc. Am.*, *78*, 1965–1983.

Besson, J. C., and P. Hamm (1983), Port de Pointe-à-Pitre: Reconnaissance géologique et géotechnique de zones de draguage et de dépôt, *Rep. 83 ANT 002*, Bur. de Rech. Géol. et Min., Orléans, France.

Bloom, A. L., W. S. Broecker, J. M. Chappell, R. K. Matthews, and K. J. Mesolella (1974), Quaternary sea level fluctuations on a tectonic coast: New $^{230}Th/^{234}U$ dates from Huon Peninsula, New Guinea, *Quat. Res.*, *4*, 185–205.

Bouysse, P., and F. Garrabé (1984), Evolution tectonique néogène des îles calcaires de l'archipel de la Guadeloupe, *C. R. Acad. Sci., Ser. II*, *298*, 763–766.

Bouysse, P., and D. Westercamp (1990), Subduction of Atlantic aseismic ridges and late Cenozoic evolution of the Lesser Antilles island arc, *Tectonophysics*, *175*, 349–380.

Bouysse, P., F. Garrabé, T. Mauboussin, P. Andreieff, R. Battistini, P. Carlier, F. Hinschberger, and J. Rodet (1993), Carte géologique du département de la Guadeloupe. Notice explicative: Marie-Galante et îlets de la Petite-Terre, scale 1:50, 000, Bur. de Rech. Géol. et Min., Orléans, France.

Bowin, C. (1976), Caribbean gravity field and plate tectonics, *Spec. Pap. Geol. Soc. Am.*, *169*, 79 pp.

Broecker, W. S., D. L. Thurber, J. Goddard, T. L. Ku, R. K. Matthews, and K. J. Mesolella (1968), Milankovitch hypothesis supported by precise dating of coral reefs and deep-sea sediments, *Science*, *159*, 297–300.

Chappell, J. (1974), Geology of coral terraces, Huon Peninsula, New Guinea: A study of Quaternary tectonic movements and sea-level changes, *Geol. Soc. Am. Bull.*, *85*, 553–570.

DeMets, C., P. E. Jansma, G. S. Mattioli, T. H. Dixon, F. Farina, R. Bilham, E. Calais, and P. Mann (2000), GPS geodetic constraints on Caribbean-North America plate motion, *Geophys. Res. Lett.*, *27*, 437–440.

Deplus, C., A. Le Friant, G. Boudon, J. C. Komorowski, B. Villemant, C. Harford, J. Ségouffin, and J. L. Cheminée (2001), Submarine evidence for large-scale debris avalanches in the Lesser Antilles arc, *Earth. Planet. Sci. Lett.*, *192*, 145–157.

De Reynal de Saint Michel, A. (1966), Carte géologique du département de la Guadeloupe. Feuilles de St Martin, St Barthelemy et Tintamarre; Basse-Terre et les Saintes; Marie-Galante et La Désirade, scale 1/50,000, Minist. de l'Ind., Paris.

Dziewonski, A. M., G. Ekstrom, and N. N. Maternovskaya (2000), Centroid-moment tensor solutions for October-December, 1999, *Phys. Earth Planet. Inter.*, *121*, 205–221.

Edwards, R. L., J. H. Chen, and G. J. Wasserburg (1987), ^{238}U - ^{234}U - ^{230}Th - ^{232}Th measurements of time over the past 500,000 years, *Earth Planet. Sci. Lett.*, *81*, 175–192.

Feuillard, M. (1985), Macrosismicité de la Guadeloupe et de la Martinique, report, Inst. de Phys. du Globe de Paris, Paris.

Feuillet, N. (2000), Sismotectonique des Petites Antilles. Liaison entre activité sismique et volcanique, thesis, 283 pp., Univ. Paris 7, Paris.

Feuillet, N., I. Manighetti, and P. Tapponnier (2001), Extension active perpendiculaire à la subduction dans l'arc des Petites Antilles (Guadeloupe), *C. R. Acad. Sci., Ser. II*, *333*, 583–590.

Feuillet, N., I. Manighetti, P. Tapponnier, and E. Jacques (2002), Arc parallel extension and localization of volcanic complexes in Guadeloupe, Lesser Antilles, *J. Geophys. Res.*, *107*, 2331, doi:10.1029/2001JB000308.

Gallup, C. D., R. L. Edwards, and R. G. Johnson (1994), The timing of high sea levels over the past 200,000 years, *Science*, *263*, 796–800.

Garrabé, F., and C. Paulin (1984), Découverte par forage de calcaires à Polypiers Pléistocène sous le Piedmont volcano-sédimentaire du Nord-Est de la Basse-Terre de Guadeloupe: Principaux résultats scientifiques et techniques, 72 pp., Bur. de Rech. Géol. et Min., Orléans, France.

Garrabé, F., P. Andreieff, P. Bouysse, and J. Rodet (1988), Notice explicative de la carte géologique de Grande-Terre, département de la Guadeloupe, scale 1:50,000, Bur. de Rech. Géol. et Min., Orléans, France.

Girardin, N., M. Feuillard, and J. P. Viodé (1990), Réseau régional sismique de l'arc des Petites Antilles: Sismicité superficielle (1981–1988), *Bull. Soc. Geol. Fr.*, *162*, 1003–1015.

Grellet, B., and B. Sauret (1988), Géomorphologie et niveaux marins des îles calcaires de l'archipel de la Guadeloupe. Implications pour l'évaluation de l'aléa sismique à l'échelle régionale et à l'échelle locale, *Rep. 88 SGN 256 GEG*, 53 pp., Bur. de Rech. Géol. et Min., Orléans, France.

Guilcher, A., and A. Marec (1978), Le récif barrière et le lagon du Grand Cul-de-sac Marin (Guadeloupe, Antilles Françaises): Géomorphologie et sediments, *Oceanol. Acta*, *1*, 435–444.

Henderson, G. M., and N. C. Slowey (2000), Evidence from U-Th dating against Northern Hemisphere forcing of the penultimate deglaciation, *Nature*, *404*, 61–65.

Imbrie, J., J. D. Hays, D. G. Martinson, A. McIntyre, A. C. Mix, J. J. Morley, N. G. Pisias, W. L. Prell, and N. J. Shackelton (1984), The orbital theory of Pleistocene climate: Support from a revised chronology of the marine $\delta^{18}O$ record, in *Milankovitch and Climate*, part I, edited by A. Berger et al., pp. 269–305, D. Reidel, Norwell, Mass.

Jacques, E., C. Monaco, P. Tapponnier, L. Tortorici, and T. Winter (2001), Faulting and earthquake triggering during the 1783 Calabria seismic sequence, *Geophys. J. Int.*, *147*, 499–516.

Kanamori, H. (1977), The energy release in great earthquakes, *J. Geophys. Res.*, *83*, 2981–2987.

King, G., and M. Ellis (1991), The origin of large local uplift in extensional regions, *Nature*, *348*, 689–693.

King, G. C. P., R. S. Stein, and J. B. Rundle (1988), The growth of geological structures by repeated earthquakes: 1. Conceptual framework, *J. Geophys. Res.*, *93*, 13,307–13,318.

Ku, T. L., M. Ivanovich, and S. Luo (1990), U series dating of the last interglacial high sea stands: Barbados revisited, *Quat. Res.*, *33*, 129–147.

Lajoie, K. R. (1986), Coastal tectonics, in *Active Tectonics*, pp. 95–124, Natl. Acad. of Sci., Washington, D. C.

Lasserre, G. (1961), La Guadeloupe, thesis, Univ. de Bordeaux 1, Talence, France.

Manighetti, I., P. Tapponnier, P. Y. Gillot, E. Jacques, V. Courtillot, R. Armijo, J. C. Ruegg, and G. C. P. King (1998), Propagation of rifting along the Arabia-Somalia plate boundary: Into Afar, *J. Geophys. Res.*, *103*, 4947–4974.

McCann, W. R., J. W. Dewey, A. J. Murphy, and S. T. Harding (1982), A large normal-fault earthquake in the overriding wedge of the Lesser

Antilles subduction zone: The earthquake of 8 October 1974, *Bull. Seismol. Soc. Am.*, *72*, 251–262.

Mesollela, K. J., R. K. Matthews, W. S. Broecker, and D. L. Thurber (1969), The astronomical theory of climatic change: Barbados data, *J. Geol.*, *77*, 250–274.

Okada, Y. (1985), Surface deformation due to shear, and tensile faults in a half-space, *Bull. Seismol. Soc. Am.*, *75*, 1135–1154.

Okada, Y. (1992), Internal deformation due to shear and tensile faults in a half-space, *Bull. Seismol. Soc. Am.*, *82*, 1018–1040.

Robson, G. (1964), An earthquake catalog for the eastern Caribbean 1530–1960, *Bull. Seismol. Soc. Am.*, *54*, 785–832.

Sainte-Claire Deville, C. (1843), Observations sur le tremblement de terre éprouvé à la Guadeloupe le 8 Février 1843, Imprimerie du Gouverneur, Basse-Terre, Guadeloupe, July.

Stein, R. S., G. C. P. King, and J. B. Rundle (1988), The growth of geological structures by repeated earthquakes: 2. Field examples of continental dip-slip faults, *J. Geophys. Res.*, *93*, 13,319–13,331.

Stein, S., J. F. Engeln, and D. A. Wiens (1982), Subduction seismicity and tectonics in the Lesser Antilles arc, *J. Geophys. Res.*, *87*, 8642–8664.

Taylor, W. F., C. Frohlich, J. Lecolle, and M. Strecker (1987), Analysis of partially emerged corals and reef terraces in the central Vanuatu Arc: Comparison of contemporary coseismic and nonseismic with Quaternary vertical movements, *J. Geophys. Res.*, *92*, 4905–4933.

Thatcher, W. (1984), The earthquake deformation cycle at the Nankai Trough, southwest Japan, *J. Geophys. Res.*, *89*, 3087–3101.

Valensise, G., and S. Ward (1991), Long-term uplift of the Santa Cruz coastline in response to repeated earthquakes along the San Andreas fault, *Bull. Seismol. Soc. Am.*, *81*, 1694–1704.

Villemant, B., and N. Feuillet (2003), Dating open systems by the ^{238}U-^{234}U-^{230}Th method: Application to Quaternary reef terraces, *Earth Planet. Sci. Lett.*, *210*, 105–118.

Wells, D. L., and K. J. Coppersmith (1994), New empirical relationships among magnitude, rupture length, rupture width, rupture area, and surface displacement, *Bull. Seismol. Soc. Am.*, *84*, 974–1002.

Westercamp, D. (1980), Une méthode d'évaluation et de zonation des risques volcaniques à la Soufrière de Guadeloupe, Antilles Françaises, *Bull. Volcanol.*, *43*, 431–452.

N. Feuillet, Istituto Nazionale di Geofisica e Vulcanologia, Via di Vigna Murata 605, I-00143 Rome, Italy. (feuillet@ingv.it)

G. C. P. King and P. Tapponnier, Institut de Physique du Globe de Paris, Laboratoire de Tectonique et Mécanique de la Lithosphère, CNRS UMR7578, 4, Place Jussieu, F-75252 Paris cedex 05, France. (king@ipgp.jussieu.fr; tappon@ipgp.jussieu.fr)

I. Manighetti, Department of Earth Sciences, University of Southern California, 3651 Trousdale Parkway, Los Angeles, CA 90089, USA. (manig@usc.edu)

B. Villemant, Université Pierre et Marie Curie, Laboratoire de Géochimie des Systèmes Volcaniques, CNRS UMR 7040, 4, Place Jussieu, F-75230 Paris cedex 05, France. (villemant@ipgp.jussieu.fr)